REVIEW ARTICLE

CrossMark

Flow and heat transfer of dusty hyperbolic tangent fluid over a stretching sheet in the presence of thermal radiation and magnetic field

K. Ganesh Kumar[1*], B. J. Gireesha[1] and R. S. R. Gorla[2]

Abstract

Background: This paper explores the impact of thermal radiation on boundary layer flow of dusty hyperbolic tangent fluid over a stretching sheet in the presence of magnetic field. The flow is generated by the action of two equal and opposite. A uniform magnetic field is imposed along the y-axis and the sheet being stretched with the velocity along the x-axis. The number density is assumed to be constant and volume fraction of dust particles is neglected. The fluid and dust particles motions are coupled only through drag and heat transfer between them.

Methods: The method of solution involves similarity transformation which reduces the partial differential equations into a non-linear ordinary differential equation. These non-linear ordinary differential equations have been solved by applying Runge-Kutta-Fehlberg forth-fifth order method (RKF45 Method) with help of shooting technique.

Results: The velocity and temperature profile for each fluid and dust phase are aforethought to research the influence of assorted flow dominant parameters. The numerical values for skin friction coefficient and Nusselt number are maintained in Tables 3 and 4. The numerical results of a present investigation are compared with previous published results and located to be sensible agreement as shown in Tables 1 and 2.

Conclusion: It is scrutinized that, the temperature profile and corresponding boundary layer thickness was depressed by uplifting the Prandtl number. Further, an increase in the thermal boundary layer thickness and decrease in momentum boundary layer thickness was observed for the increasing values of the magnetic parameter.

Keywords: Boundary layer flow, Hyperbolic tangent fluid, Thermal radiation, Fluid particle suspension, Stretching sheet

Review

The main objective of the present inspection is to study the MHD flow and radiative heat transfer of hyperbolic tangent fluid over a stretching sheet with fluid-particle suspension. The method of solution involves similarity transformation which reduces the partial differential equations into a non-linear ordinary differential equation. These non-linear ordinary differential equations have been solved by applying Runge-Kutta-Fehlberg forth-fifth order method (RKF45 Method) with help of Shooting technique. The temperature and velocity profiles for various values of flow parameters are presented in the figures. The numerical results of present investigation were compared with existing results and are found to be in good agreement.

Introduction

Boundary layer flow and heat transfer under the influence of stretching surface has received considerable attention in recent years. The problem has scientific and chemical engineering applications such as aerodynamic extrusion of plastic sheets and fibers, tinning of copper wire, drawing,

* Correspondence: ganikganesh@gmail.com
[1]Department of Studies and Research in Mathematics, Kuvempu University Shankaraghatta, Shimoga 577 451, Karnataka, India
Full list of author information is available at the end of the article

crystal growing and glass blowing, annealing and paper production, metallurgical process, polymer extrusion process, continuous stretching, drawing, annealing and tinning of copper wires. Sakiadis (1961) was the pioneer of studying the boundary layer flow over a stretched surface moving under a constant velocity. Rajagopal and Gupta (1987) examined the boundary layer flow over a stretching sheet for a various class of non-Newtonian fluids. Rauta and Mishra (2014) investigated the heat transfer characteristics of two-dimensional flow in a porous medium over a stretching sheet with internal heat generation. There-after, exhaustive amount of researches were made related to boundary layer flow and heat transfer (see Ishak (2010), Ali (2006) and Yao et al. (2011)).

In recent years, many researchers are concentrated on the area of dusty fluid due to its wide range of applications such as fluidization, centrifugal separation of matter from fluid, purification of crude oil, dust collection, petroleum industry, powder technology, nuclear reactor cooling, performance of solid fuel rocket nozzles, and paint spraying. Saffman (1962) analyzed the flow of a dusty gas in which the fluid suspension particles are uniformly distributed. Further, Mohan Krishna et al. (2013) have discussed the flow of a dusty viscous fluid in the presence of transverse magnetic field with first order chemical reaction. Datta and Mishra (1982) presented the boundary layer flow of a dusty fluid over a semi-infinite flat plate along with the drag force. Due to these applications, a number of theoretical and experimental studies have been carried out by numerous researchers on dusty fluid (see (Palani and Ganesan 2007; Ramesh et al. 2017; Kumar et al. 2017a, 2017d, 2017f; Makinde et al. 2017)).

On the other hand, non-Newtonian fluids are found in many industrial and engineering processes, such as food mixing, flow of blood, plasma, mercury amalgams, and lubrications with heavy oils and greases. In view of these applications, many studies are focused on non-Newtonian fluid. Govardhan et al. (2015) initiated the magnetohydrodynamics flow of an incompressible micropolar fluid over a stretching sheet for unsteady case. Hayat et al. (2010) have initiated the effect of thermal radiation on a two-dimensional stagnation-point flow and heat transfer of an incompressible magneto-hydrodynamic Carreau fluid towards a shrinking surface with convective boundary condition. In modern days, all such interesting applications have motivated scientists and researchers to look for more avenues in the field of non-Newtonian flow (Rudraswamy et al. 2017a, 2017b; Kumar et al. 2017c, 2017e).

One of the imperative branches of non-Newtonian fluid is the tangent hyperbolic fluid capable of describing the shear thinning effects. Recently, Akbar et al. (2013) have discussed the two dimensional tangent hyperbolic fluid flow over a stretching in the presence of magnetic field.

Malik et al. (2015) have used Keller box method to study MHD flow of tangent hyperbolic fluid under the influence of stretching cylinder. Nadeem and Akram (2011) analyzed the magnetohydrodynamics (MHD) peristaltic flow of a tangent hyperbolic fluid model in a vertical asymmetric channel (Fig. 1). Recently Naseer et al. (2014) have analyzed the steady boundary layer flow and heat transfer of a tangent hyperbolic fluid flow under the influence of vertical exponentially stretching cylinder. Kumar et al. (2017b) discussed an unsteady squeezed flow of a tangent hyperbolic fluid over a sensor surface in the presence of variable thermal conductivity. Nadeem and Maraj (2013) initiated the mathematical analysis for peristaltic flow of tangent hyperbolic fluid in a curved channel.

The main objective of the present inspection is to study the MHD flow and radiative heat transfer of hyperbolic tangent fluid over a stretching sheet with fluid-particle suspension. The method of solution involves similarity transformation which reduces the partial differential equations into a non-linear ordinary differential equation. These non-linear ordinary differential equations have been solved by applying Runge–Kutta–Fehlberg fourth-fifth order method (RKF-45 Method) with the help of shooting technique. The temperature and velocity profiles for various values of flow parameters are presented in the figures. The numerical results of present investigation were compared with existing results and are found to be in good agreement.

Method
The system of non-linear ordinary differential equations (2.8)–(2.9) and (3.10)–(3.11) using the boundary conditions (2.10) and (3.12) are solved numerically using Runge–Kutta–Fehlberg fourth-fifth (RKF-45) method. In maple, two sub methods are available, namely trapezoidal and midpoint method. To solve this kind of two-point boundary value problem the trapezoidal method is generally efficient, but it is incapable to handle harmless endpoint singularities, but this can be able in midpoint
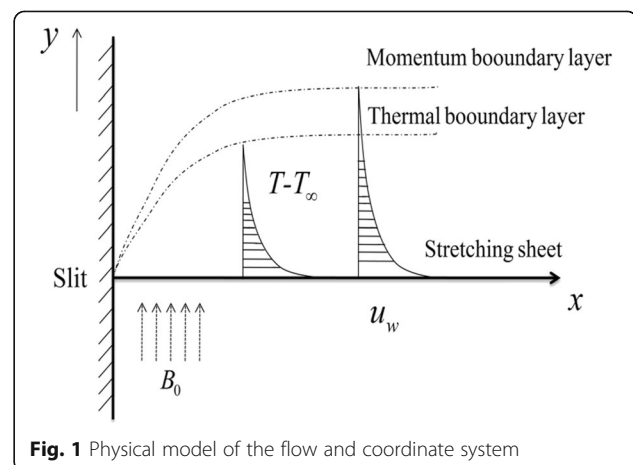
Fig. 1 Physical model of the flow and coordinate system

method. Thus, the mid-point method with the Richardson extrapolation enhancement scheme is chosen as a sub method. The asymptotic boundary conditions at η_∞ were replaced by those at $\eta_\infty = 6$ in accordance with standard practice in the boundary layer analysis. Additionally, the relative error tolerance for convergence is considered to be 10^{-6} throughout our numerical computations. The consequences of assorted pertinent parameters on flow and heat transfer characteristics are mentioned numerically and presented graphically. Comparisons between the current and former limiting results were shown in the Tables 1 and 2.

Mathematical formulation

Let us consider a steady flow of an incompressible hyperbolic tangent fluid over a stretching sheet. The flow is assumed to be confined to region of $y > 0$. The flow is generated by the action of two equal and opposite forces along the x-axis and y-axis being normal to the flow. A uniform magnetic field B_0 is imposed along the y-axis and the sheet being stretched with the velocity $u_w(x)$ along the x-axis. The number density is assumed to be constant and volume fraction of dust particles is neglected. The fluid and dust particle motions are coupled only through drag and heat transfer between them. The drag force is modeled using Stokes linear drag theory. Other interaction forces such as the virtual force, the shear lift force, and the spin-lift force will be neglected compared to the drag force. The term T_w represents the temperature of fluid at the sheet, whereas T_∞ denotes the ambient fluid temperature.

The constitutive equation of tangent hyperbolic fluid is (Akbar et al. 2013)

$$\overline{\tau} = \left[\mu_0 + (\mu_0 + \mu_\infty)\tanh\left(\Gamma\overline{\dot\gamma}\right)^n\right]\overline{\dot\gamma},$$

$$(2.1)$$

in which, $\overline{\tau}$ is the extra stress tensor, μ_∞ the infinite shear rate viscosity, μ_0 the zero shear rate viscosity, Γ is the time dependent material constant, n the power law index, i.e., flow behavior index and $\overline{\dot\gamma}$ is defined as

Table 1 Comparison table of skin friction coefficient ($We = n = 0$)

M	Akbar et al. (2013) (RKF-45 method)	Fathizadeh et al. (2013) (HAM method)	Present result (RKF-45 method)
1	− 1.41421	− 1.41421	− 1.41421
5	− 2.44948	− 2.44948	− 2.44949
10	− 3.31662	− 3.31662	− 3.31662
50	− 7.14142	− 7.14142	− 7.14143
500	− 22.3830	− 22.3830	− 22.38302
1000	− 31.6386	− 31.6386	− 31.63858

Table 2 Comparison of $-\theta'(0)$ for different values of Prandtl number (Pr) when $M = 0$, $We = 0$, $n = 0$, Ec = 0, and $R = 0$

Pr	Ali (2006) (RK-45 method)	Chen (1998) (Finite difference method)	Present (RKF-45 method)
1.0	− 0.5801	− 0.58199	− 0.58223
3.0	− 1.1599	− 1.16523	− 1.16522
5.0	–	–	− 1.56803
10.0	− 2.2960	− 2.30796	− 2.30798
100.0	–	–	− 7.76564

$$\overline{\dot\gamma} = \frac{1}{2}\sqrt{\frac{1}{2}\sum_i\sum_j\overline{\dot\gamma}_{ij}\,\overline{\dot\gamma}_{ji}} = \sqrt{\frac{1}{2}\Pi}.$$

Consider Eq. (2.1), for the case when $\mu_\infty = 0$, because it is not possible to discuss the problem for infinite shear rate viscosity and since we have considered tangent hyperbolic fluid that describing shear thinning effects so $\Gamma\overline{\dot\gamma} < 1$. Then, Eq. (2.1) takes the form

$$\overline{\tau} = \mu_0\left[\left(\Gamma\overline{\dot\gamma}\right)^n\right],$$

$$= \mu_0\left[1 + n\left(\Gamma\overline{\dot\gamma} - 1\right)\right]\overline{\dot\gamma}$$

Governing equations for hyperbolic tangent fluid model after applying the boundary layer approximations can be defined as follows (Hayat et al. 2010; Rudraswamy et al. 2017a):

$$\frac{\partial u}{\partial x} + \frac{\partial v}{\partial y} = 0, \qquad (2.2)$$

$$u\frac{\partial u}{\partial x} + v\frac{\partial u}{\partial y} = \nu(1-n)\frac{\partial^2 u}{\partial y^2} + \sqrt{2}\nu n\Gamma\left(\frac{\partial u}{\partial y}\right)\frac{\partial^2 u}{\partial y^2}$$
$$+ \frac{KN}{\rho}(u_p - u) - \frac{\sigma B_0^2}{\rho}u, \qquad (2.3)$$

$$\frac{\partial u_p}{\partial x} + \frac{\partial v_p}{\partial y} = 0, \qquad (2.4)$$

$$\rho_p\left(u_p\frac{\partial u_p}{\partial x} + v_p\frac{\partial u_p}{\partial y}\right) = KN(u - u_p),$$

$$(2.5)$$

where (u, u_p) and (v, v_p) are the velocity components in x and y directions of the fluid and dust particle phase, respectively. ρ and $\rho_p = mN$ are the densities of the fluid and dust particle phase, respectively. m and N are the mass and number density of the dust particles per unit volume, respectively. σ is the electrical conductivity of the fluid, ν is the kinematic viscosity of the base fluid, μ is the coefficient of viscosity of the fluid, $K = 6\pi\mu r$ is the Stokes drag coefficient, and r is the radius of dust particle.

Ganesh Kumar *et al. International Journal of Mechanical and Materials Engineering* (2018) 13:2

Page 4 of 11

The appropriate boundary conditions applicable to the present problem are

$$u = u_w(x), \quad v = 0 \quad \text{at } y = 0,$$
$$u \to 0, \quad u_p \to 0, \quad v_p \to v \text{ as } y \to \infty,$$

$$(2.6)$$

where $u_w(x) = bx$ is a stretching sheet velocity with b (>0) as the stretching rate.

Equations (2.2) to (2.5) subjected to boundary conditions (2.6) admits self-similar solution in terms of the similarity function f, F and similarity variable η and they are defined as

$$u = bxf'(\eta), v = -\sqrt{vb}f(\eta), \eta = \sqrt{\frac{b}{v}}y,$$
$$u_p = bxF'(\eta), v_p = -\sqrt{vb}F(\eta),$$
$$(2.7)$$

the Eq. (2.2) and (2.4) are identically satisfied, in terms of relations (2.7). In addition, the equation (2.3) and (2.5) are reduced to the following set of non-linear ordinary differential equations:

$$(1-n)f'''(\eta) - [f'(\eta)]^2 + f''(\eta)f(\eta) + nW_e f'''(\eta)f''(\eta)$$
$$+ l\beta_v[F'(\eta) - f'(\eta)] - Mf'(\eta) = 0,$$
$$(2.8)$$

$$F(\eta)F''(\eta) - [F'(\eta)]^2 + \beta_v[f'(\eta) - F'(\eta)] = 0. \quad (2.9)$$

Transformed boundary conditions are

$$f' = 1, f(\eta) = 0 \quad \text{at } \eta = 0,$$
$$f'(\eta) \to 0 F'(\eta) \to 0, F(\eta) \to f(\eta) \text{ as } \eta \to \infty,$$
$$(2.10)$$

where $l = \frac{Nm}{\rho}$ is the mass concentration parameter of dust particles, $M = \frac{\sigma B_o^2}{\rho b}$ is the magnetic parameter, $\tau_v = \frac{m}{K}$ is the relaxation time of the dust particles, $\beta_v = \frac{1}{b\tau_v}$ is the fluid-particle interaction parameter for velocity, $W_e = \frac{\sqrt{2b\Gamma}u_w}{\sqrt{v}}$ is the Weissenberg number, and n is the power law index parameter.

Heat transfer analysis

The governing boundary layer heat transport equations for both fluid and dust phase are given by

$$c_p\rho(u\frac{\partial T}{\partial x} + v\frac{\partial T}{\partial y}) = k\frac{\partial^2 T}{\partial y^2} + \frac{\rho_p C_p}{\tau_T}(T_p - T) + \frac{\rho_p}{\tau_v}(u_p - u)^2$$
$$- \frac{\partial q_r}{\partial y},$$
$$(3.1)$$

$$u_p\frac{\partial T_p}{\partial x} + v_p\frac{\partial T_p}{\partial y} = -\frac{c_p}{c_m\tau_T}(T_p - T), \quad (3.2)$$

where T and T_p are the temperature of the fluid and dust particles, respectively, c_p and c_m are the specific heat of fluid and dust particles, respectively, τ_T is the thermal equilibrium time, i.e., the time required by the dust cloud to adjust its temperature to that of fluid, k is the thermal conductivity of the fluid, and q_r is the radiative heat flux.

Using the Rosseland approximation for radiation, radiation heat flux is simplified as

$$q_r = -\frac{4\sigma^*}{3k^*}\frac{\partial T^4}{\partial y},$$
$$(3.3)$$

where σ^* is the Stefan–Boltzmann constant and k^* is the mean absorption coefficient. It is noted that the optically thick radiation limit is considered in this model. Assuming that the temperature differences within the flow are sufficiently small such that T^4 may be expressed as a linear function of temperature, we expand T^4 in a Tayler series about T_∞ as follows:

$$T^4 = T_\infty^4 + 4T_\infty^3(T - T_\infty) + 6T_\infty^2(T - T_\infty)^2 + ...,$$
$$(3.4)$$

neglect the higher order terms beyond the first degree in $(T - T_\infty)$, one can get,
$$T^4 \cong 4T_\infty^3 T - 3T_\infty^4. \quad (3.5)$$

Substituting Eq. (3.5) in Eq. (3.3) one can get,

$$\frac{\partial q_r}{\partial y} = -\frac{16\sigma^* T_\infty^3}{3k^*}\frac{\partial^2 T}{\partial y^2}. \quad (3.6)$$

In view of the Eq. (3.6), the energy Eq. (3.1) becomes

$$c_p\rho(u\frac{\partial u}{\partial x} + v\frac{\partial v}{\partial y}) = (k + \frac{16\sigma^* T_\infty^3}{3k^*})\frac{\partial^2 T}{\partial y^2} + \frac{\rho_p C_p}{\tau_T}(T_p - T)$$
$$+ \frac{\rho_p}{\tau_v}(u_p - u)^2.$$
$$(3.7)$$

Corresponding boundary conditions for the temperature are considered as follows:

Ganesh Kumar *et al. International Journal of Mechanical and Materials Engineering* (2018) 13:2

Page 5 of 11

Table 3 Numerical values of $-\sqrt{Re}C_f$ and $-\left[\frac{Nu_x}{Re^{1/2}}\right]$ for different values of W_e, n, M, β_v, and l

M	W_e	β_v	l	n	$-\sqrt{Re}C_f$	$-\left[\frac{Nu_x}{Re^{1/2}}\right]$
0					1.0547	1.0506
0.5					1.2641	1.0115
1					1.4446	0.9788
	0				1.2247	1.0137
	0.3				1.2641	1.0115
	0.6				1.3057	1.0093
		0.5			1.2641	1.0115
		1			1.2958	0.9956
		1.5			1.3144	0.9834
			0.5		1.2641	1.0115
			1		1.3268	1.1973
			1.5		1.3868	1.3598
				0	1.2440	1.1973
				0.1	1.2909	1.0257
				0.2	1.3268	0.9942

$$T = T_w \text{ at } y = 0 \quad \begin{array}{l} T \to T_\infty, \, T_p \to T_\infty \end{array} \text{ as } y \to \infty$$

$$(3.8)$$

The dimensional fluid phase temperature $\theta(\eta)$ and dust phase temperature $\theta_p(\eta)$ are defined as

Table 4 Numerical values of $-\left[\frac{Nu_x}{Re^{1/2}}\right]$ for different values of Ec, γ, Pr, R, and β_t

Ec	γ	Pr	R	β_t	$-\left[\frac{Nu_x}{Re^{1/2}}\right]$
0					1.0175
0.1					0.9581
0.2					0.8987
	1				0.9633
	2				0.9049
	3				0.8718
		2			0.7834
		3			1.0115
		4			1.2055
			0		1.3770
			0.5		1.0115
			1		0.8188
				0.5	0.9833
				1	1.1007
				1.5	1.1786

$$\theta(\eta) = \frac{T - T_\infty}{T_w - T_\infty}, \quad \theta_p(\eta) = \frac{T_p - T_\infty}{T_w - T_\infty}.$$

$$(3.9)$$

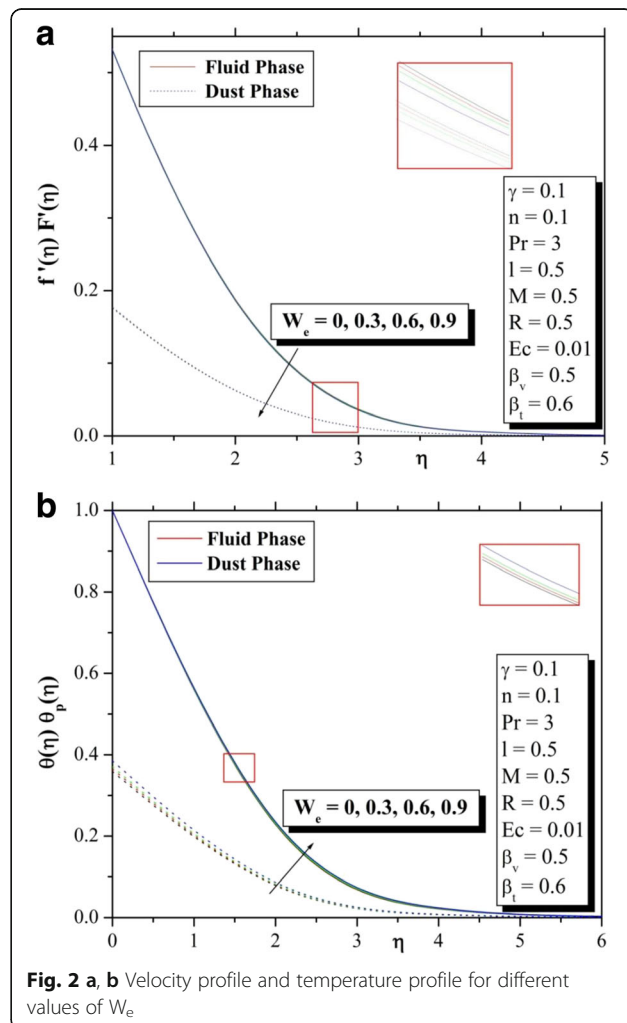Using (3.9) into (3.7) and (3.2), one can get the following non-linear ordinary differential equations:

$$\left(1 + \frac{4}{3}R\right)\theta''(\eta) + \text{Pr}\theta'(\eta)f(\eta) + lPr\beta_t\big(\theta_p(\eta) - \theta(\eta)\big)$$

$$+ \beta_v l \text{EcPr}\big[F'(\eta) - f'(\eta)\big]^2 = 0,$$

$$(3.10)$$

$$\theta_{p'}(\eta)F(\eta) - \gamma\beta_t\big[\theta_p(\eta) - \theta(\eta)\big] = 0, \qquad (3.11)$$

with

$$\theta(\eta) = 1 \text{ at } \quad \eta = 0,$$
$$\theta(\eta) \to 0, \quad \theta_p(\eta) \to 0 \quad as \, \eta \to \infty,$$

$$(3.12)$$

where $\text{Pr} = \frac{\mu C_p}{k}$ is Prandtl number, the prime denote differentiation with respect to η and $\frac{R = 4\sigma^* T_\infty^3}{k^* k}$ is the

Fig. 2 a, b Velocity profile and temperature profile for different values of W_e

radiation parameter, $Ec = \frac{u_w^2}{c_p(T_w - T_\infty)}$ is the Eckert number, $\gamma = \frac{c_p}{c_m}$ is the specific heat ratio, $\beta_t = \frac{1}{b\tau_T}$ is the fluid-particle interaction parameter for temperature.

The physical quantities of interest like skin friction coefficient (C_f) and local Nusselt number (Nu_x) are defined as

$$c_f = \frac{\tau_w}{\rho u_w^2} \text{ and } Nu_x = \frac{u_w q_w}{ak(T_\infty - T_w)}$$

where the shear stress (τ_w) and surface heat flux (q_w) are given by

$$\tau_w = \mu_0\left((1-n)\frac{\partial u}{\partial y} + \frac{n\Gamma}{\sqrt{2}}\left(\frac{\partial u}{\partial y}\right)^2\right) \text{ and } q_w$$

$$= -k\frac{\partial T}{\partial y} + q_r.$$

Using the non-dimensional variables, one can get

$$\sqrt{Re}\,C_f = \left[(1-n)f''(\eta) + \frac{n}{2}W_e\big(f''(\eta)\big)^2\right]_{\eta=0} \quad (3.14)$$

$$\text{and } \frac{Nu_x}{\sqrt{Re_x}} = -\left(1 + \frac{4}{3}R\right)\theta'(0),$$

where $Re_x = \frac{u_w^2}{av}$ is the local Reynold's number.

Result and discussion

In the current paper, we have investigated the impact of thermal radiation on the boundary layer flow of dusty hyperbolic tangent fluid over a stretching sheet with applied magnetic field. The velocity and temperature profile for each fluid and dust phase are aforethought to research the influence of assorted flow dominant parameters like magnetic parameter, Prandtl number, Eckert number, specific heat ratio, Weissenberg number, thermal radiation parameter, power law index, and fluid-particle interaction parameter. The numerical values for skin friction coefficient and Nusselt number are
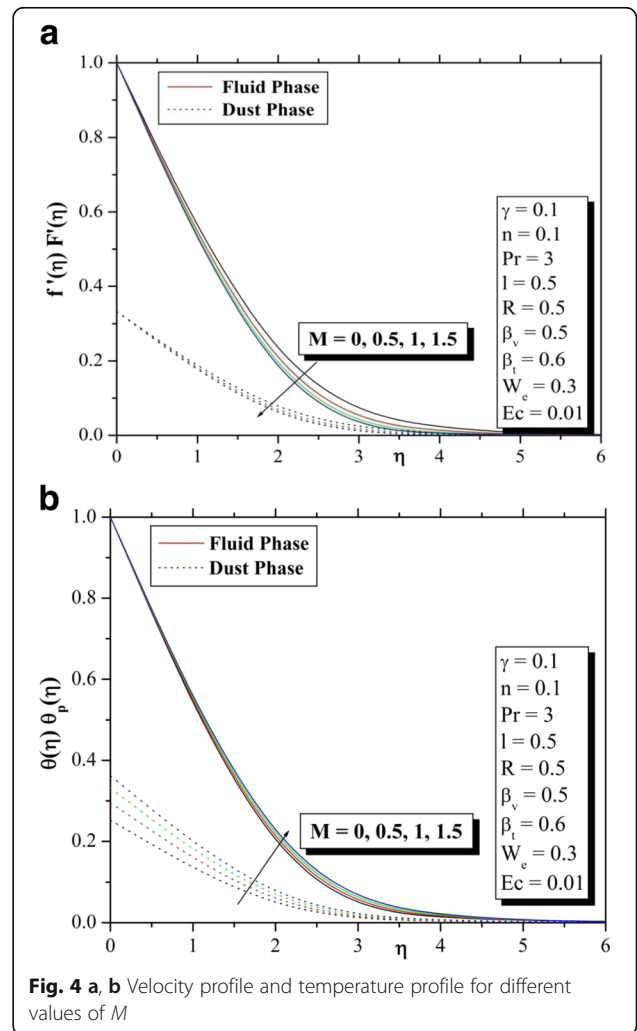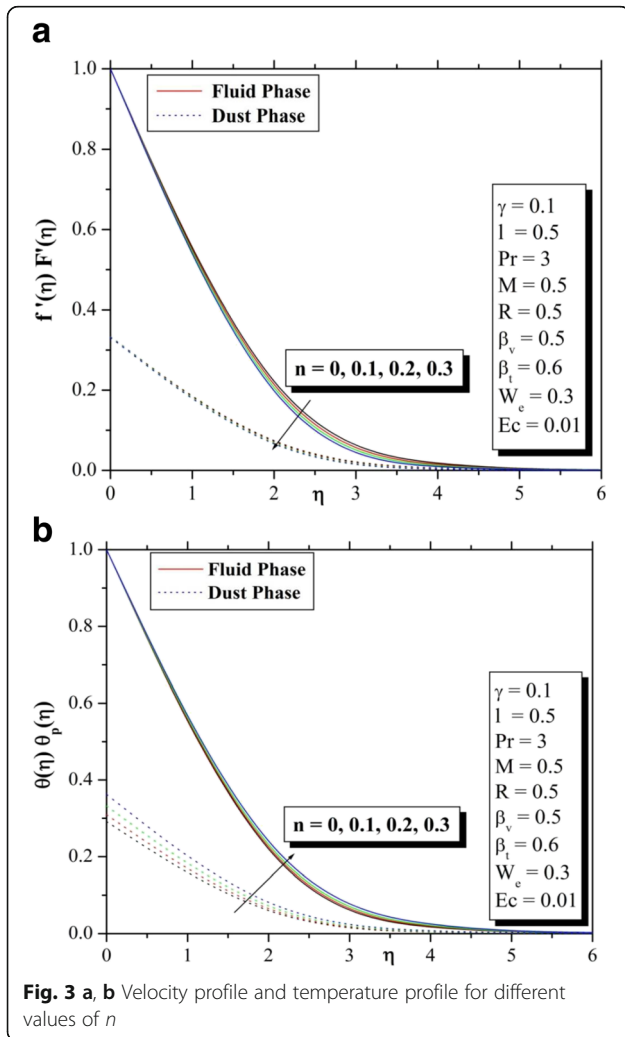
Fig. 3 a, b Velocity profile and temperature profile for different values of n

Fig. 4 a, b Velocity profile and temperature profile for different values of M

maintained in Tables 3 and 4. The numerical results of a present investigation are compared with previous published results and located to be sensible agreement as shown in Tables 1 and 2.

Figure 2a, b describes the impact of Weissenberg number (W_e) over the velocity and temperature profile. Weissenberg number is the quantitative relation of the relaxation time of the fluid and a particular process time. This ratio will increase the thickness of the fluid, thus, velocity profile and also the associated boundary layer thickness decreases with increase of W_e in shown in Fig. 2a. In the case of the temperature profile, it exhibits the opposite behavior of velocity profile as in Fig. 2b.

Figure 3a, b depicts the behavior of power law index (n) on velocity and temperature profile. Figure 3a exposes that the velocity profile and corresponding boundary layer thickness decreases by increasing the values of power law index parameter (n). Figure 3b emphasizes the temperature distribution for various values of power law

index parameter. From this figure, temperature profile is strongly depressed with increasing power law index.

The velocity and temperature profiles are pictured in Fig. 4a, b for the variation of a magnetic parameter (M). In general, an application of transverse magnetic field normal to the flow of an electrically conducting fluid has the affection to yield a drag-like force called the Lorentz force, which acts in the direction opposite to that of flow, thus reducing its velocity. The results also show that momentum boundary layer thickness decreases whereas thermal boundary layer thickness increases.

The variations of velocity and temperature profile for both the phases are illustrated in Fig. 5a, b for various values of β_v and β_t. An uplifting value of β_v can decrease the fluid phase velocity and will increase the dust phase velocity. While, evidently, an increase in β_t can increase the dust phase and reduce the fluid phase temperature profile. This is because of the presence of dust particles produces friction force in the fluid, which retards the flow.

Fig. 5 a, b Velocity profile and temperature profile for different values of β_v and β_t

Fig. 6 a, b Velocity profile and temperature profile for different values of l
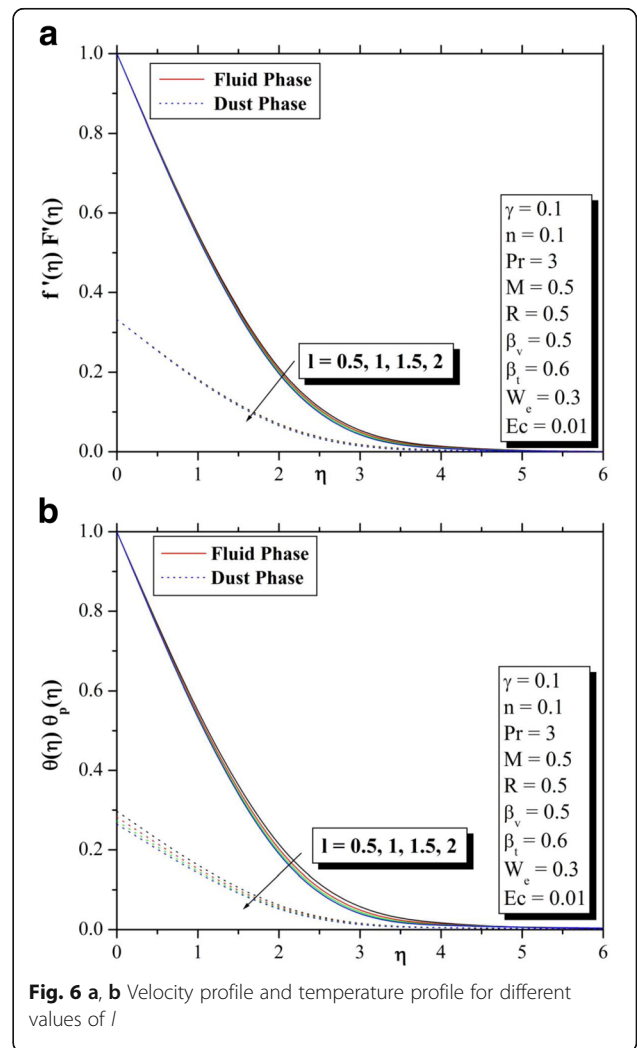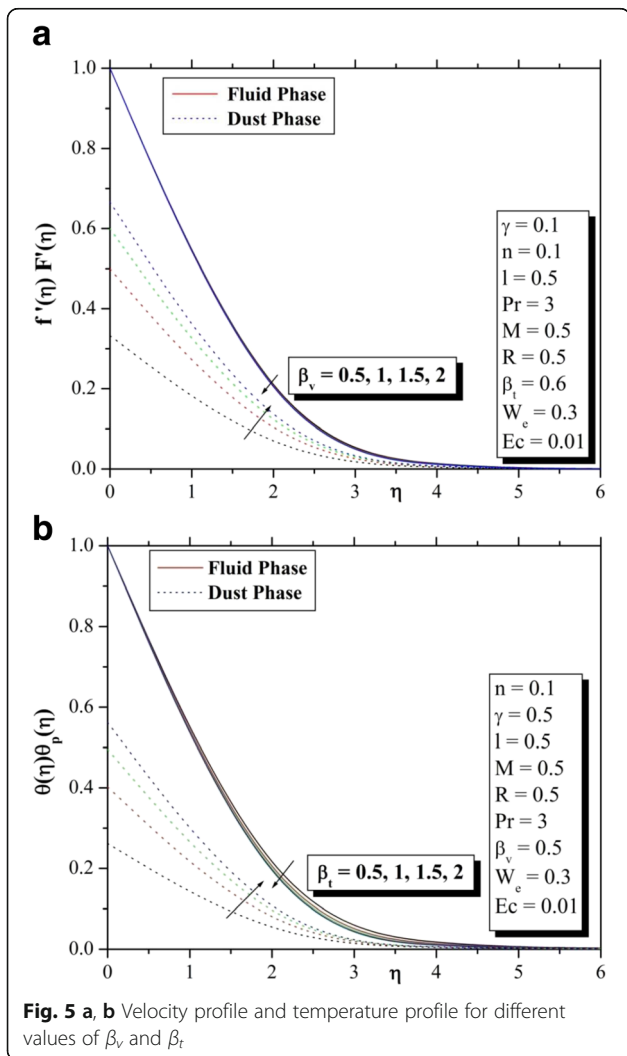
Figure 6a, b shows the impact of l on velocity and temperature profiles for each fluid and particle phases. Once the dust particles are suspended within the clean fluid, an interior friction is created at intervals in the fluid, and additionally, the dust particles absorb heat from the fluid once they acquire contact. As a result, thinning of thermal boundary layer thickness takes place. This tends to scale back the velocity and temperature profiles of both phases with the increase in dust particle parameter.

Figures 7a, 7b, and 8a depict the temperature profiles for various values of Eckert number (Ec), specific heat ratio (γ), and radiation parameter (R), respectively. One can infer from these figures that the temperature and thickness of the corresponding boundary layer of both phases will increase with rising in Ec, γ, and R. Here, Fig. 8a, determines that the effect of radiation is also to enhance the heat transfer. Thus, radiation should be at its minimum in order to facilitate the cooling process. Figure 8b describes the impact of Prandtl number (Pr) over the temperature profile. Hear the thermal boundary layer thickness
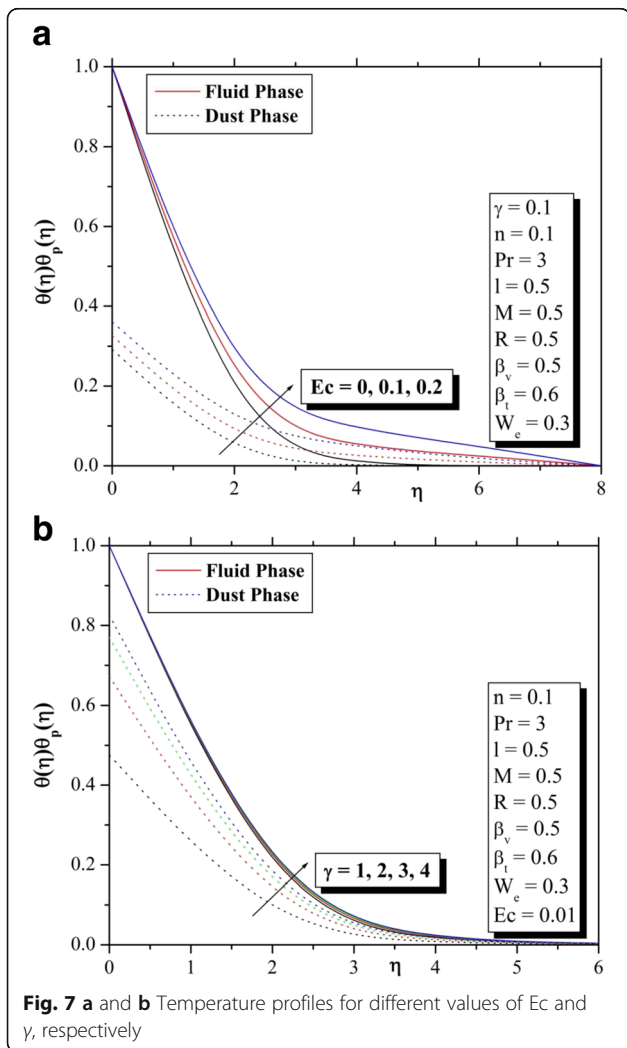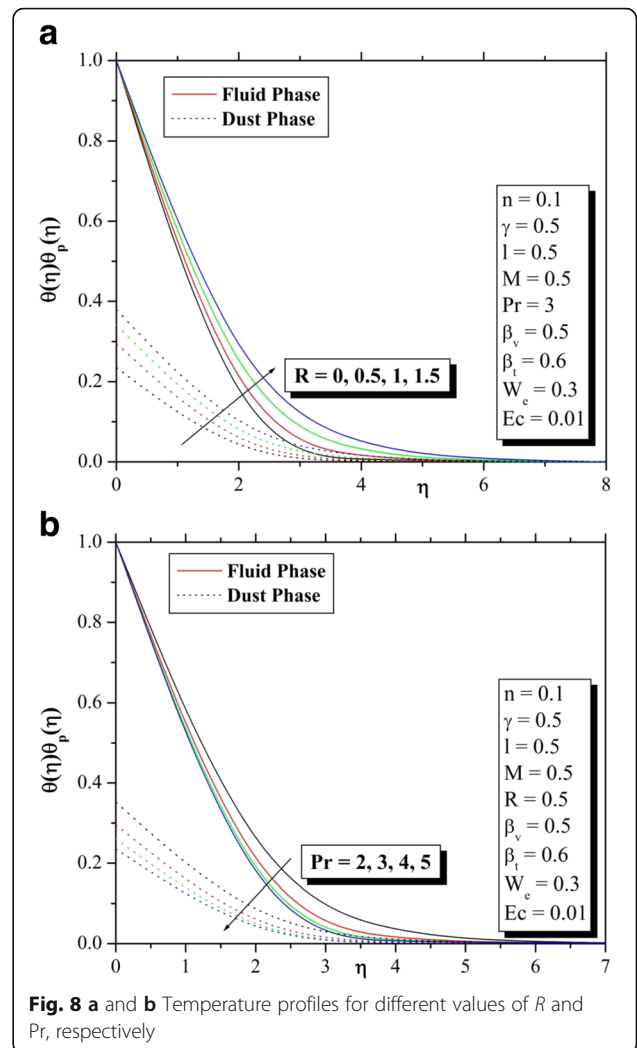

Fig. 8 a and **b** Temperature profiles for different values of R and Pr, respectively

minimizes by maximizing the values of Prandtl number. The central reason for reduction in temperature is a higher Prandtl number has relatively low thermal conductivity, which causes low heat penetration, thus the thermal boundary layer thickness of fluid and dust particles decreases with the rise in Prandtl number.

Figure 9a–c depicts the skin friction coefficient for β_v, n, and We with different values of l, M, and l, respectively. It is obvious that skin friction coefficient will increase with associate rising values of β_v, n, and W_e versus l, M, and l, respectively. In Fig. 10a, b, it determined that the Nusselt number decrease with increasing values of γ and R versus Ec and γ, respectively. However, Nusselt number while increase by increasing the values of Pr and β_t versus R and l, respectively. This is shown in Fig. 10c, d.

Table 3 presents the numerical values of Nusselt number and skin friction coefficient for various values M, W_e, β_v. It is observed that skin friction increase and Nusselt number decreases with increasing M, W_e, β_v, l, and n. Table 4 presents the numerical values of

Fig. 7 a and **b** Temperature profiles for different values of Ec and γ, respectively
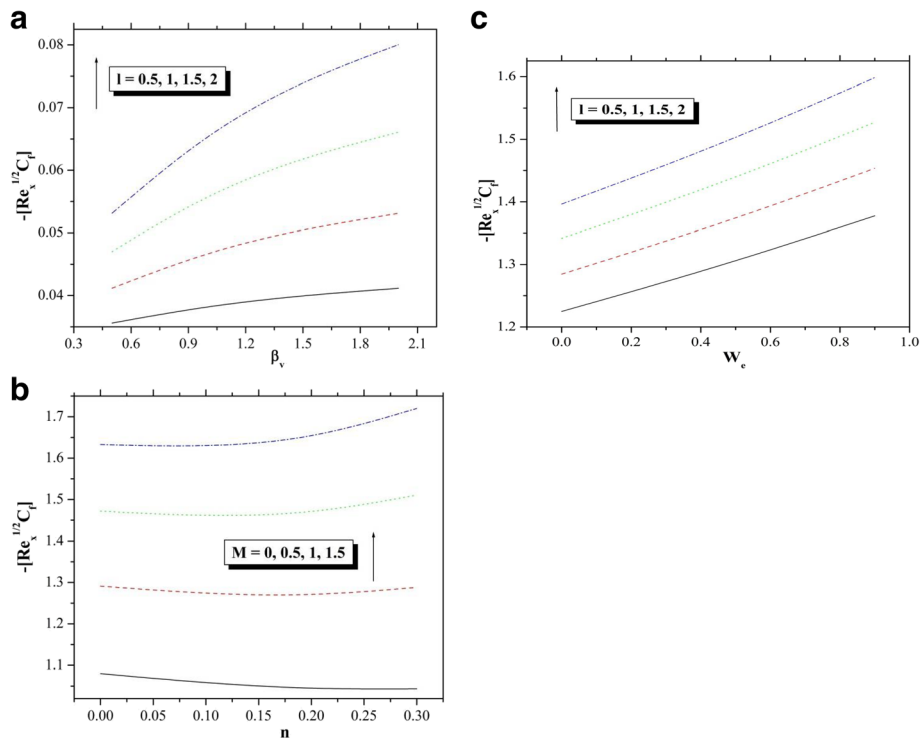
Fig. 9 a Influence of β_v and *l* on skin friction. **b** Influence of *n* and *M* on skin friction. **c** Influence of *n* and *M* on skin friction
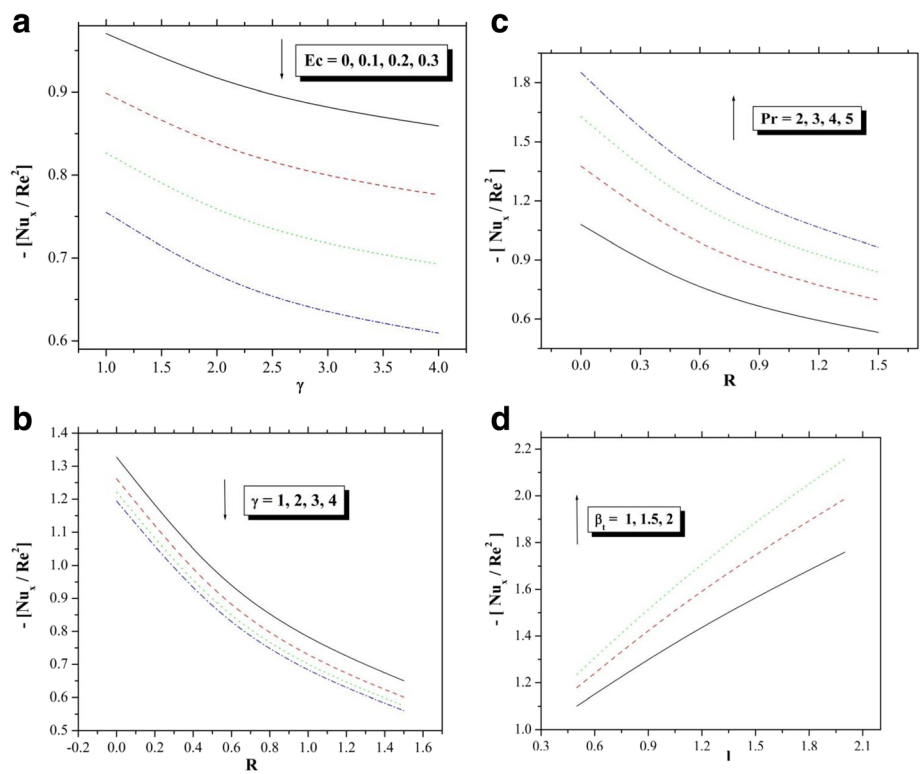
Fig. 10 a Influence of Ec and γ on Nusselt number. **b** Influence of *R* and γ on Nusselt number. **c** Influence of *R* and Pr on Nusselt number. **d** Influence of *l* and β_t on Nusselt number

local Nusselt number for various values Ec, γ, Pr, R, and β_t. From this table, we observed that, Nusselt number increase with an increasing the values of Pr and β_t whereas an opposite trend is observed for different values Ec, γ, and R.

Conclusions

The present work includes the impact of thermal radiation on boundary layer flow of dusty hyperbolic tangent fluid over a stretching sheet underneath the influence of magnetic field. Numerical results are conferred in tabular/ graphical kind to elucidate the details of flow and heat transfer characteristics and their dependence on the varied physical parameters. The subsequent conclusions are drawn:

- Increasing values of W_e and n will increase the temperature profile. However, decrease the velocity profile.
- An increasing values of Ec, γ, and R parameters increase the thermal boundary layer thickness.
- The temperature profile and corresponding boundary layer thickness was depressed by uplifting the Prandtl number.
- Velocity and temperature profiles decreases by an increasing values of l.
- With a rise of β_v and β_t, velocity and temperature profile decreases for fluid phase, but increases for dust phase.
- An increase in the thermal boundary layer thickness and decrease in momentum boundary layer thickness was observed for the increasing values of the magnetic parameter M.

Nomenclature

B_0^2 magnetic field
b stretching rate
c_p fluid phase specific heat coefficient (J/kgK)
c_m dust phase specific heat coefficient (J/kgK)
C_f skin friction coefficient
Ec Eckert number
f dimensionless velocity of the fluid phase
F dimensionless velocity of the dust phase
K Stokes drag constant
k thermal conductivity
k^* mean absorption coefficient (m^{-1})
l mass concentration of dust particles parameter
M magnetic parameter
m mass of dust particles
n power law index
N dust particles number density
Nu_x local Nusselt number
Pr Prandtl number

q_w heat flux at the surface
q_r radiative heat flux (Wm^{-2})
R radiation parameter
r radius of dust particles
Re_x local Reynolds number
Sh_x Sherwood number
T temperature of the fluid phase
T_p temperature of the dust phase
T_w temperature of the fluid at the sheet
T_∞ ambient fluid temperature
u_w stretching sheet velocity
u, u_p velocity components of fluid phase
v, v_p velocity components of dust phase
W_e Weissenberg number
x coordinate along the plate (m)
y coordinate normal to the plate (m)

Greek symbols

β_v fluid-particle interaction parameter for velocity
β_t fluid-particle interaction parameter for temperature
μ dynamic viscosity ($kgm^{-1}s^{-1}$)
ν kinematic viscosity
σ electrical conductivity of the fluid
σ^* Stefan-Boltzmann constant
θ temperature of the fluid phase
θ_p temperature of the dust phase
η similarity variable
τ_T thermal equilibrium time
τ_w surface shear stress
τ_v dust particles relaxation time
γ specific heat ratio
ρ base fluid density (kg/m^3)
ρ_p dust particles density
Γ the time constant

Superscript:

$'$ derivative with respect to η

Subscript:

p particle phase
∞ fluid properties at ambient condition.

Competing interests
The authors declare that they have no competing interests.

Publisher's Note

Springer Nature remains neutral with regard to jurisdictional claims in published maps and institutional affiliations.

Ganesh Kumar *et al. International Journal of Mechanical and Materials Engineering* (2018) 13:2

Page 11 of 11

Author details
[1]Department of Studies and Research in Mathematics, Kuvempu University Shankaraghatta, Shimoga 577 451, Karnataka, India. [2]Department of Mechanical and Civil Engineering, Purdue University Northwest, Westville, Indiana 46391, USA.

References
Akbar, NS, Nadeem, S, Haq, RU, Khan, ZH. (2013). Numerical solutions of magneto hydrodynamic boundary layer flow of tangent hyperbolic fluid flow towards a stretching sheet with magnetic field. *Indian Journal of Physics*, *87*(11), 1121–1124.
Ali, ME. (2006). The effect of variable viscosity on mixed convection heat transfer along a vertical moving surface. *International Journal of Thermal Sciences*, *45*, 60–69.
Chen, CH. (1998). Laminar mixed convection adjacent to vertical continuously stretching sheets. *Heat and Mass Transfer*, *33*, 471–476.
Datta, N, & Mishra, SK. (1982). Boundary layer flow of a dusty fluid over a semi-infinite flat plate. *Acta Mechanica*, *42*, 71–83.
Fathizadeh, M, Madani, M, Khan, Y, Faraz, N, Yildirim, A, Tutkun, S. (2013). An effective modification of the homotopy perturbation method for MHD viscous flow over a stretching sheet. *Journal of King Saud University-Science*, *25*(2), 107–113.
Govardhan, K, Nagaraju, G, Kaladhar, K, Balasiddulu, M. (2015). MHD and radiation effects on mixed convection unsteady flow of micropolar fluid over a stretching sheet. *Procedia Computer Science*, *57*, 65–76.
Hayat, T, Saleem, N, Ali, N. (2010). Effect of induced magnetic field on peristaltic transport of a Carreau fluid. *Communications in Nonlinear Science and Numerical Simulation*, *15*(9), 2407–2423.
Ishak, A. (2010). Similarity solutions for flow and heat transfer over a permeable surface with convective boundary condition. *Applied Mathematics and Computation*, *217*, 837–842.
Kumar, GK, Gireesha, BJ, Rudraswamy, NG, Gorla, RSR. (2017a). Melting heat transfer of hyperbolic tangent fluid over a stretching sheet with fluid particle suspension and thermal radiation. *Communications in Numerical Analysis*, *2*(2017), 125–140.
Kumar, KG, Gireesha, BJ, Krishnamurthy, MR, Rudraswamy, NG. (2017b). An unsteady squeezed flow of a tangent hyperbolic fluid over a sensor surface in the presence of variable thermal conductivity. *Results in Physics*, *7*, 3031–3036.
Kumar, KG, Gireesha, BJ, Manjunatha, S, Rudraswamy, NG. (2017c). Effect of nonlinear thermal radiation on double-diffusive mixed convection boundary layer flow of viscoelastic nanofluid over a stretching sheet. *International Journal of Mechanical and Materials Engineering*, *12*(1), 18.
Kumar, KG, Gireesha, BJ, Rudraswamy, NG, Manjunatha, S. (2017d). Radiative heat transfers of Carreau fluid flow over a stretching sheet with fluid particle suspension and temperature jump. *Results in Physics*, *7*, 3976–3983.
Kumar, KG, Rudraswamy, NG, Gireesha, BJ, Krishnamurthy, MR. (2017e). Influence of nonlinear thermal radiation and viscous dissipation on three-dimensional flow of Jeffrey nano fluid over a stretching sheet in the presence of joule heating. *Nonlinear Engineering*, *6*(3), 207–219.
Kumar, KG, Rudraswamy, NG, Gireesha, BJ, Manjunatha, S. (2017f). Non linear thermal radiation effect on Williamson fluid with particle-liquid suspension past a stretching surface. *Results in Physics*, *7*, 3196–3202.
Makinde, OD, Kumar, KG, Manjunatha, S, Gireesha, BJ. (2017). Effect of nonlinear thermal radiation on MHD boundary layer flow and melting heat transfer of micro-polar fluid over a stretching surface with fluid particles suspension. *Defect and Diffusion Forum*, *378*, 125–136.
Malik, MY, Salahuddin, T, Hussain, A, Bilal, S. (2015). MHD flow of tangent hyperbolic fluid over a stretching cylinder: using Keller box method. *Journal of Magnetism and Magnetic Materials*, *395*, 271–276.
Mohan Krishna, P, Sugunamma, V, Sandeep, N. (2013). Magnetic field and chemical reaction effects on convective flow of dusty viscous fluid. *Communications in Applied Sciences*, *1*, 161–187.
Nadeem, S, & Akram, S. (2011). Magneto hydrodynamic peristaltic flow of a hyperbolic tangent fluid in a vertical asymmetric channel with heat transfer. *Acta Mechanica Sinica*, *27*(2), 237–250.
Nadeem, S, & Maraj, EN. (2013). The mathematical analysis for peristaltic flow of hyperbolic tangent fluid in a curved channel. *Communications in Theoretical Physics*, *59*, 729–736.
Naseer, M, Malik, MY, Nadeem, S, Rehman, A. (2014). The boundary layer flow of hyperbolic tangent fluid over a vertical exponentially stretching cylinder. *Alexandria Engineering Journal*, *53*, 747–750.
Palani, G, & Ganesan, P. (2007). Heat transfer effects on dusty gas flow past a semi-infinite inclined plate. *Forsch Ingenieurwes (Springer)*, *71*, 23–230.
Rajagopal, KR, & Gupta, AS. (1987). A non-similar boundary layer on a stretching sheet in a non-Newtonian fluid with uniform free stream. *Journal of Mathematical and Physical Sciences*, *21*(2), 189–200.
Ramesh, GK, Kumar, KG, Shehzad, SA, Gireesha, BJ. (2018). Enhancement of radiation on hydromagnetic Casson fluid flow towards a stretched cylinder with suspension of liquid-particles. *Canadian Journal of Physics*, *96*(1): 18-24.
Rauta, AK, & Mishra, SK. (2014). Heat transfer of a dusty fluid over a stretching sheet with internal heat generation/absorption. *International Journal of Engineering & Technology*, *03*(12), 28–41.
Rudraswamy, NG, Kumar, KG, Gireesha, BJ, Gorla, RSR. (2017a). Soret and Dufour effects in three-dimensional flow of Jeffery nanofluid in the presence of nonlinear thermal radiation. *Journal of Nanoengineering and Nanomanufacturing*, *6*(4), 278–287.
Rudraswamy, NG, Kumar, KG, Gireesha, BJ, Gorla, RSR. (2017b). Combined effect of joule heating and viscous dissipation on MHD three dimensional flow of a Jeffrey nanofluid. *Journal of Nanofluids*, *6*(2), 300–310.
Saffman, PG. (1962). On the stability of laminar flow of a dusty gas. *Journal of Fluid Mechanics*, *13*, 120–128.
Sakiadis, BC. (1961). Boundary layer behavior on continuous solid surface; boundary layer equation for two dimensional and axisymmetric flow. *AICHE Journal*, *7*, 26–28.
Yao, S, Fang, T, Zhong, Y. (2011). Heat transfer of a generalized stretching/shrinking wall problem with convective boundary conditions. *Communications in Nonlinear Science and Numerical Simulation*, *16*, 752–760.